Range-Doppler Resolution in Subarray-MIMO Radar with Modified Barker Code: Performance Comparison with PA and MIMO Radars

Aji Trisna Bhakti[1], Syahfrizal Tahcfulloh[2]
Department of Electrical Engineering, Universitas Borneo Tarakan
Jl. Amal Lama, No. 1, Tarakan 77123, Indonesia
Email: syahfrizal@borneo.ac.id*

ARTICLE INFORMATION

Received 23 July 2024
Revised 06 February 2025
Accepted 11 February 2025

Keywords:
Ambiguity function
Barker code
Hadamard code
MIMO radar
Subarrays

A B S T R A C T

The type of transmission signal in the telecommunications sector, especially for radar-communication-system-applications, plays an important role in determining the success of system performance. The desired waveform is a signal that has high autocorrelation with minimum-sidelobes, especially for radar-applications that are used to detect targets and minimize of interference and interceptions. Many waveforms have been used in this application, one of which is the Barker code. This paper evaluates and analyzes the use of the modified code for subarray-multiple-input multiple-output (SMIMO) radar applications, which exhibit adaptive detection performance based on target and environmental conditions, an aspect not explored in previous studies. The ambiguity function (AF) performance of this waveform is used to obtain range-Doppler-resolution with three-dimensional plot as function of time-delay, angle, and Doppler frequency. AF performance was tested involving the mainlobe-sidelobe level, peak-sidelobe-ratio (PSLR), and number of transmit subarrays in the SMIMO radar which were compared with the performance of conventional radars such as phased-array (PA) and MIMO radars. For example, the self-modified Barker code ($B_{11,7}$) gives mainlobe AF performance on PA, MIMO, and SMIMO (K = 5) radars of 48.86dB, 53.86dB, and 54.75dB, respectively. Meanwhile, range resolution, Doppler resolution, and PSLR are 214.5m, 1402.65m/s, and -8.449dB respectively.

1. Introduction

The use of transmitted waveforms in the telecommunications sector, especially for the integration of communications and radar systems, is a hot and interesting topic that continues to be researched. Regarding the advantages of the communication system-radar integration, a waveform is needed which on the communication system side is superior in providing data rates with low symbol error rates while on the radar system side it provides a high signal-to-interference-plus-noise-ratio so that it can minimizing the influence of interference and disturbing noise (Nusenu et al., 2018). According to Sturm & Wiesbeck (2011), the combination of a radar-communication system produces an intelligent signaling system that can function as ad-hoc communication and at the same time as remote sensing, thereby reducing costs and making spectrum allocation more efficient. By transmitting waveform pulses from this combination of systems, multi-directional communication capabilities and target detection can be obtained simultaneously, which are presented in bit error rates and multi-dimensional ambiguity functions (Wu et al., 2023). On the other hand, the development of the 5G communication system also supports MIMO communication which requires waveform transmission that has spectrum efficiency, resistance to interference, and reliable beamforming (Admaja, 2018).

Based on several existing researches, there are several types of waveforms that have been implemented in combined radar-communication systems and for other applications, one of which is Barker code. This code has several advantages such as: in radar applications it has been reported that this code is proven to have low interception and strong anti-jamming capabilities (Aziz et al., 2024; Wang & He, 2018) and helps in the

DOI:10.17933/bpostel.v23i1.400

development of a versatile waveform generator capable of adapts to carrier frequencies and wide bandwidth so that it has the opportunity to have high range resolution (Dhawan & Choudhary, 2023), in opto-electronics communication applications that this code has a forward error correction threshold requirement of around 7% for non-line-of-sight channels (NLOS) at a distance of 5 m (Dong et al., 2023), in certain communication system applications that this code is resistant and resistant to noise (Riznvk et al., 2021), in 5G cellular network systems it has been reported that with the application of this code it occurs improvement in uplink energy efficiency for various signal-to-noise ratio (SNR) conditions (Aljalai et al., 2020), in Global Positioning System (GPS) system applications, it has been stated that this code helps in improving aperiodic autocorrelation properties (Matsuyuki & Tsuneda, 2018), and others. On the other hand, this code can also be applied to support low packet-loss-rate communications as reported by Ni'amah et al. (2020) with its coded-random-access.

Based on the description of the advantages of the Barker code as a transmission waveform, this paper examines it in more depth and analyzes the use of this code, especially for radars that employ many antennas at the transmitter (Tx) and many antennas at the receiver (Rx), known as multiple-input multiple-output (MIMO) radar to support multiple target detection performance. This was raised because from several studies that have been previously reported, there is relatively no one who has directly studied and evaluated the application of this code to MIMO radars, especially those that apply the subarray method to their antenna systems. However, this code has been used in MIMO radars without subarrays as investigated by Aljalai et al. (2020), Dhawan & Choudhary (2023), and Wang & He (2018). Meanwhile, according to several studies regarding subarrays, this technique has advantages, including: enlarging the virtual antenna array which results in high detection angle resolution and minimizing grating lobes (Han & Hong, 2022; Tahcfulloh, 2021), being able to suppress jammers, increasing estimation resolution angle (Jiazhi et al., 2017), lowering cost, and computation (Elayaperumal & Hari, 2019), increasing degree-of-freedom (DOF), and reducing mutual coupling thereby improving array estimation performance (Lai et al., 2024), and others. Leveraging the advantages of the Barker code and its potential for subarray-MIMO (SMIMO) radar, this study fills a gap left by previous research by providing a comprehensive and detailed evaluation and analysis.

In evaluating the performance of using waveforms on radar, there is one method that is commonly used, i.e. ambiguity function (AF). According to Tang et al. (2019) that AF can analyze the relationship or correlation between the transmission waveform and the signal received by the radar originating from the target in the form of range-Doppler resolution parameters of the radar. AF can also be used to analyze appropriate waveforms to improve radar detection by providing minimum sidelobe levels (Farnane & Minaoui, 2021). So far, especially for MIMO radar applications, AF has been implemented but has not been applied for SMIMO radar and especially those that use Barker code, such as: for distributed MIMO radar systems where AF is a function of SNR (Ilioudis et al., 2016), the use of phase code sequences to provide AF performance in function of the level of the weighted integrated sidelobe and the level of the peak sidelobe (Wei & Wei, 2023), the use of Phased-Costas coded waveforms to minimize range-doppler sidelobes and target cross-correlation of AF with limited bandwidth (Celik & Tuncer, 2023), the use of AF equipped with the multiple-signal-classification-alternating-projection (MUSIC-AP) estimation method to increase the estimation resolution for detection and imaging capabilities (Li et al., 2023), and so on. In a study conducted by Sabaria & Tahcfulloh (2024), the use of subarrays and linear-frequency-modulated waveform (LFM) in MIMO radar to increase range and speed resolution has been reported, potentially combined with the waveform proposed in this paper.

Therefore, this paper presents key insights not covered in previous studies, particularly on AF using a modified Barker code waveform specifically applied to SMIMO radar. The AF performance of the SMIMO radar with this waveform will be presented in a three-dimensional plot, i.e. as a function of time-delay, Doppler frequency, and target angle. Meanwhile, the parameters of the proposed AF radar that are analyzed include sidelobe-mainlobe level, peak-sidelobe-ratio (PSLR), number of subarrays in Tx, and comparison with other types of conventional radar such as PA and MIMO radar.

2. Literature review

Below is a description of AF. AF is a tool that is commonly applied to evaluate and analyze transmission signals from radar (Mahafza, 2002). AF is a function of time delay (t_d) and Doppler frequency (f_D). Based on the AF of the bit vector sequence signal, $\boldsymbol{\varphi}[n]$ reported byhafza (2002) and for $\boldsymbol{\varphi}[n]$ in this paper using those listed in Table 1, the Barker code is expressed as a matrix of AF, i.e., $\boldsymbol{\Psi}(t_d,f_D)$. Next, the matrix $\boldsymbol{\Psi}(t_d,f_D)$ is implemented into the AF of the SMIMO radar system to obtain processing gain from the use of an antenna array in the Tx-Rx.

Table 1. Barker Code for Bit Length Variation

Type	Bit length (n)	Sequence of bit vectors, $\boldsymbol{\varphi}[n]$
B_2	2	[+1 -1] or [+1 +1]
B_3	3	[+1 +1 -1]
B_4	4	[+1 -1 +1 +1] or [+1 -1 -1 -1]
B_5	5	[+1 +1 +1 -1 +1]
B_7	7	[+1 +1 +1 -1 -1 +1 -1]
B_{11}	11	[+1 +1 +1 -1 -1 -1 +1 -1 -1 +1 -1]
B_{13}	13	[+1 +1 +1 +1 +1 -1 -1 +1 +1 -1 +1 -1 +1]

Barker code has been widely implemented in combined radar-communication systems and various other applications, demonstrating several advantages. In radar applications, it is recognized for its low interception and strong anti-jamming capabilities (Aziz et al., 2024; Wang & He, 2018), and contributes to developing versatile waveform generators that adapt to carrier frequencies and wide bandwidth, enabling high range resolution (Dhawan & Choudhary, 2023). Additionally, it is resistant to noise in certain communication systems (Riznvk et al., 2021), and in 5G cellular networks, it has been shown to improve uplink energy efficiency under various signal-to-noise ratio (SNR) conditions (Aljalai et al., 2020). For GPS systems, Barker code enhances aperiodic autocorrelation properties (Matsuyuki & Tsuneda, 2018). Furthermore, it supports low packet-loss-rate communications, as reported by Ni'amah et al. (2020), with its coded-random-access capabilities.

To optimize AF performance and PSLR, choose code configurations based on radar environment and target characteristics (Friedlander, 2007). In high-clutter or interference settings, select codes like modified Barker or Hadamard to minimize sidelobe levels for improved detection. In low-clutter scenarios, opt for flexible codes offering higher range and velocity resolution. For closely spaced targets, prioritize codes that enhance range and Doppler resolution, such as modified Barker codes (Kim et al., 2021). When dealing with multiple targets at varying speeds, use combinations of Barker, Hadamard, or MIMO-based codes for fine resolution in both range and velocity.

3. Method

Several things related to the research method carried out in this paper include: First, the modified Barker code and its AF; Second, determining the expression for the AF of the SMIMO radar using the code; Third, several stages are described for evaluating the AF of the SMIMO radar based on these waveforms, and fourth, to evaluate the AF performance according to several values of all the parameters used in this study.

3.1. *Ambiguity Function of the Modified Barker Code*

The waveform of this modified Barker code is used to modulate the carrier signal emitted by the radar system. According to Levanon & Mozeson (2004), to obtain minimum PSLR, low sidelobe levels and a series of pulses from the waveform that have high energy, Kronecker product ($\otimes$) can be applied with the bit sequence between the codes (B_n) or with other codes such as Hadamard (H_n) (Tahcfulloh & Hendrantoro, 2016). The following is a calculation of the Kronecker product between a 2-bit Barker code (B_2) and a 7-bit Barker code (B_7) which produces a 14-bit sequence of bits in $B_{2,7}$, i.e.,

[+1 -1]$\otimes$[+1 +1 +1 -1 -1 +1 -1] = [+1 +1 +1 -1 -1 +1 -1 -1 -1 -1 +1 +1 -1 +1] ……………………………………1)

Meanwhile, the Kronecker product between B_7 and B_2 produces a 14-bit sequence of bits in $B_{7,2}$, i.e.,

[+1 +1 +1 -1 -1 +1 -1]$\otimes$[+1 -1] = [+1 -1 +1 -1 +1 -1 -1 +1 -1 +1 +1 -1 -1 +1] ……………………………………2)

For the Kronecker product between 2-bit Barker code (B_2) and 8-bit Hadamard (H_8), a 16-bit sequence is produced in B_2H_8, i.e.,

[+1 -1]$\otimes$[+1 -1 -1 +1 -1 +1 +1 -1] = [+1 -1 -1 +1 -1 +1 +1 -1 -1 +1 +1 -1 +1 -1 -1 +1] …………………………3)

Meanwhile, the Kronecker product between H_8 and B_2 produces a 16-bit sequence in H_8B_2, namely

[+1 -1 -1 +1 -1 +1 +1 -1]$\otimes$[+1 -1] = [+1 -1 -1 +1 -1 +1 +1 -1 -1 +1 +1 -1 +1 -1 -1 +1] …………………………4)

Furthermore, a modified Barker code has been obtained with several types of codes which are presented respectively in Tables 2 and 3, namely between Barker codes ($B_{m,n}$) which have different bit lengths and between these codes and Hadamard (B_mH_n or H_mB_n).

Table 2. The Bit Sequence for the Modified Barker Code with Itself

Type	Bit length (n)	Sequence of bit vectors, $\varphi[n]$
$B_{2,11}$	22	[+1 +1 +1 -1 -1 -1 +1 -1 -1 +1 -1 -1 -1 -1 +1 +1 +1 -1 +1 +1 -1 +1]
$B_{11,2}$	22	[+1 -1 +1 -1 +1 -1 -1 +1 -1 +1 -1 +1 +1 -1 -1 +1 -1 +1 +1 -1 -1 +1]
$B_{3,13}$	39	[+1 +1 +1 +1 +1 -1 -1 +1 +1 -1 +1 -1 +1 +1 +1 +1 +1 +1 -1 -1 +1 +1 -1 +1 -1 +1 -1 -1 -1 -1 -1 +1 +1 -1 -1 +1 -1 +1 -1]
$B_{13,3}$	39	[+1 +1 -1 +1 +1 -1 +1 +1 -1 +1 +1 -1 +1 +1 -1 -1 -1 +1 -1 -1 +1 +1 +1 -1 +1 +1 -1 -1 -1 +1 +1 +1 -1 -1 -1 +1 +1 +1 -1]
$B_{5,13}$	65	[+1 +1 +1 +1 +1 -1 -1 +1 +1 -1 +1 -1 +1 +1 +1 +1 +1 +1 -1 -1 +1 +1 -1 +1 -1 +1 +1 +1 +1 +1 +1 -1 -1 +1 +1 -1 +1 -1 +1 -1 -1 -1 -1 -1 +1 +1 -1 -1 +1 -1 +1 -1 +1 +1 +1 +1 +1 -1 -1 +1 +1 -1 +1 -1 +1]
$B_{13,5}$	65	[+1 +1 +1 -1 +1 +1 +1 +1 -1 +1 +1 +1 +1 -1 +1 +1 +1 +1 -1 +1 +1 +1 +1 -1 +1 -1 -1 -1 +1 -1 -1 -1 -1 +1 -1 +1 +1 +1 -1 +1 +1 +1 +1 -1 +1 -1 -1 -1 +1 -1 +1 +1 +1 -1 +1 -1 -1 -1 +1 -1 +1 +1 +1 -1 +1]
$B_{7,11}$	77	[+1 +1 +1 -1 -1 -1 +1 -1 -1 +1 -1 +1 +1 +1 -1 -1 -1 +1 -1 -1 +1 -1 +1 +1 +1 -1 -1 -1 +1 -1 -1 +1 -1 -1 -1 -1 +1 +1 +1 -1 +1 +1 -1 +1 -1 -1 -1 +1 +1 +1 -1 +1 +1 -1 +1 +1 +1 +1 -1 -1 -1 +1 -1 -1 +1 -1 -1 -1 -1 +1 +1 +1 -1 +1 +1 -1 +1]
$B_{11,7}$	77	[+1 +1 +1 -1 -1 +1 -1 +1 +1 +1 -1 -1 +1 -1 +1 +1 +1 -1 -1 +1 -1 -1 -1 -1 +1 +1 -1 +1 -1 -1 -1 +1 +1 -1 +1 -1 -1 -1 +1 +1 -1 +1 +1 +1 +1 -1 -1 +1 -1 -1 -1 -1 +1 +1 -1 +1 -1 -1 -1 +1 +1 -1 +1 +1 +1 +1 -1 -1 +1 -1 -1 -1 -1 +1 +1 -1 +1

Table 3. Sequence of Bits for Modified Barker Code with Hadamard Code

Type	Bit length (n)	Sequence of bit vectors, $\boldsymbol{\varphi}[n]$
B_5H_4	20	[+1 -1 -1 +1 +1 -1 -1 +1 +1 -1 -1 +1 -1 +1 +1 -1 +1 -1 -1 +1]
H_4B_5	20	[+1 +1 +1 -1 +1 -1 -1 -1 +1 -1 -1 -1 -1 +1 -1 +1 +1 +1 -1 +1]
B_7H_4	28	[+1 -1 -1 +1 +1 -1 -1 +1 +1 -1 -1 +1 -1 +1 +1 -1 -1 +1 +1 -1 +1 -1 -1 +1 -1 +1 +1 -1]
H_4B_7	28	[+1 +1 +1 -1 -1 +1 -1 -1 -1 -1 +1 +1 -1 +1 -1 -1 -1 +1 +1 -1 +1 +1 +1 +1 -1 -1 +1 -1]
B_5H_8	40	[+1 -1 -1 +1 +1 -1 -1 +1 +1 -1 -1 +1 +1 -1 -1 +1 +1 -1 -1 +1 +1 -1 -1 +1 -1 +1 +1 -1 -1 +1 +1 -1 +1 -1 -1 +1 +1 -1 -1 +1]
H_8B_5	40	[+1 +1 +1 -1 +1 -1 -1 -1 +1 -1 -1 -1 -1 +1 -1 +1 +1 +1 -1 +1 +1 +1 +1 -1 +1 -1 -1 -1 +1 -1 -1 -1 -1 +1 -1 +1 +1 +1 -1 +1]
B_7H_8	56	[+1 -1 -1 +1 +1 -1 -1 +1 +1 -1 -1 +1 +1 -1 -1 +1 +1 -1 -1 +1 +1 -1 -1 +1 -1 +1 +1 -1 -1 +1 +1 -1 -1 +1 +1 -1 -1 +1 +1 -1 +1 -1 -1 +1 +1 -1 -1 +1 -1 +1 +1 -1 -1 +1 +1 -1]
H_8B_7	56	[+1 +1 +1 -1 -1 +1 -1 -1 -1 -1 +1 +1 -1 +1 -1 -1 -1 +1 +1 -1 +1 +1 +1 +1 -1 -1 +1 -1 +1 +1 +1 -1 -1 +1 -1 -1 -1 -1 +1 +1 -1 +1 -1 -1 -1 +1 +1 -1 +1 +1 +1 +1 -1 -1 +1 -1]

3.2. *Ambiguity Function of Modified Barker Code for SMIMO Radar*

The ambiguity function for the SMIMO radar in the direction of arrival of the signal θ to the Rx antenna is formulated according to the AF determination of the MIMO radar by Chen & Vaidyanathan (2008) and the AF determination of the Phased-MIMO radar by Khan et al. (2014). After the AF expression from the SMIMO radar is obtained, it is continued to evaluate the effectiveness of its performance by comparing it to the AF performance of conventional radars such as the PA and the MIMO radars. AF performance is carried out by involving factors such as time delay, Doppler shift, target angle, and number of Tx subarrays. The following is the AF of the SMIMO radar which is expressed as

$$|\Phi(t_d, f_D, \theta)|^2 = |\sqrt{(M/K)}\ \mathbf{b}^T(\theta)\boldsymbol{\Psi}(t_d, f_D)[\mathbf{c}(\theta)\odot\mathbf{d}(\theta)]|^2 \quad \text{………………………………………5)}$$

where M and K respectively represent the number of antennas in Tx and the number of subarrays in Tx, $\boldsymbol{\Psi}(t_d,f_D)$ is the AF matrix of the transmission signal for the modified Barker code measuring $M \times K$, $\odot$ is the Hadamard multiplication operator on vectors, $\mathbf{c}(\theta)$ and $\mathbf{d}(\theta)$ according to Tahcfulloh (2021) are vectors of coherent processing and waveform diversity formed by subarrays in Tx. Based on Equation 5, it can be interpreted that the magnitude of the AF for the SMIMO radar is determined by combinations of the number of Tx subarrays (K) which are represented by $\mathbf{c}(\theta)\odot\mathbf{d}(\theta)$. However, what determines the range-velocity resolution of Equation 5 is not the number of Tx subarrays but is determined by the type of waveform used in the radar system, which in this case is the modified Barker code.

As a comparison, the AF expression for MIMO radar is also given with slight modifications as reported by Chen & Vaidyanathan (2008), i.e.,

$$|\Phi(t_d, f_D, \theta)|^2 = |\ \mathbf{b}^T(\theta)\boldsymbol{\Psi}(t_d, f_D)\mathbf{a}(\theta)|^2 \quad \text{………………………………………………………6)}$$

where for MIMO radar the number of subarrays is $K = M$ and each Tx antenna element transmits M waveforms with transmit steering vector $\mathbf{a}(\theta)$.

3.3. *AF Radar SMIMO Determination Process for Modified Barker Code*

The following is the process for evaluating the AF performance of the modified Barker code on the SMIMO radar including:

3.3.1. *Determination of Range-Velocity Resolution and PSLR from Modified Barker Code*

To evaluate AF from this waveform, the AF expression adopted from Mahafza (2002) for Barker signals is used. The resulting AF plot includes AF as a function of time delay and Doppler frequency, AF as a function of $t_d = 0$, and AF as a function of $f_D = 0$. Next, to determine the resolution range (Δ_R) and speed (Δ_V) of the AF it is assumed that the system radar frequency (f_c) at 10 GHz in the X-band. If the velocity of light in a vacuum $c = 3\times10^8$ m/s^2, then the range resolution and velocity are respectively expressed by

$$\Delta_R = \frac{ct_d}{2} \qquad \text{...7)}$$

and

$$\Delta_R = \frac{cf_D}{2f_c} \qquad \text{...8)}$$

where it really depends on the signal bandwidth (B).

PSLR is the comparison between the square of the level for the maximum sidelobe magnitude ($M_{SL,0}$) and the square of the level for the mainlobe magnitude (M_{ML}). Determination of PSLR from the modified Barker code is determined by (Johnson et al., 2016)

$$\gamma = \frac{1}{M_{ML}^2} max\{M_{SL,0}^2\} \qquad \text{...9)}$$

The Barker code was modified with various variations, including a combination with the Hadamard code, to achieve an optimal compromise and maximize its potential for obtaining the best Δ_R, Δ_V, and PSLR for implementation in SMIMO radar.

3.3.2. *Comparison of AF Performance between SMIMO Radar and Conventional Radar*

Determining the AF of a SMIMO radar with a modified Barker code waveform can use Equation 5 which is compared with the AF performance of a PA and MIMO radar whose formulation has been given by Chen & Vaidyanathan (2008).

3.3.3. *Determination of AF from Modified Barker Code for SMIMO Radar with Varying Number of Tx Subarrays (K)*

Determination of AF from this waveform by varying the number of subarrays (K) on the SMIMO radar can use Equation 5 where $k = 1, 2, ..., M$.

3.4. *Parameters for AF Evaluation of SMIMO Radar*

Some of the assumed parameters used in this paper to evaluate the AF of the modified Barker code on the proposed radar are summarized in Table 4 where M and N denote the total number of antennas in the Tx-Rx, λ denotes the wavelength of the working frequency (f_c), the spacing between the antenna elements at Tx and Rx are d_M and d_N, respectively. All these parameters are given to meet the consideration of real conditions and practical radar applications as has been done by Mahafza (2002) and for AF radar SMIMO has been investigated by Sabaria & Tahcfulloh (2024) for LFM code. Table 4 gives the ranges for the three-dimensional plots of AF on SMIMO radars such as t_d, f_d, dan θ.

Table 4. Parameter Assumptions in AF Evaluation of Modified Barker Code for SMIMO Radar

Parameter	Value
t_d (μs)	[-63, +63]
f_D (MHz)	[-0.065, +0.065]
$M = N$	10
K	$1 \leq K \leq 10$
f_c (GHz)	10
λ (m)	0.03
d_M, d_N	0.5λ
θ (deg)	[-90, 90]

4. Result and Discussion

In this section, the results of the AF performance evaluation of this waveform for the SMIMO radar are given, following the steps in Section 3.3 and using the parameters shown in Section 3.4 or in Table 4. After the results are given, it is continued with a detailed discussion.

4.1. *AF Performance for Modified Barker Code*

After carrying out the steps from Section 3.3.1, several results will be obtained which are displayed successively in Figures 1, 2, and 3 for: AF performance for Barker code waveform in Table 1, AF performance for modified Barker code between $B_m \otimes B_n$ or $B_{m,n}$ in Table 2, and AF performance for modified Barker code with Hadamard code, i.e., $B_m \otimes H_n$ in Table 3.

4.1.1. *Original Barker Code*

First, the AF results from the Barker code without modification are given as a comparison with the AF performance for the modified Barker code. For the performance results of this AF, an example is given in B_{13} which is shown in Figure 1. In general, the AF from this code has a relatively low sidelobe level with several sidelobes. Based on Figure 1(c), which is in the form of AF as a function of $f_D = 0$, we can then determine t_d and the level of the first sidelobe ($M_{SL,0}$) so that the resolution range and PSLR (γ) can be determined. In Figure 1(c) it is known that the mainlobe touches the t_d axis for the first time at ±0.09686μs, thus obtaining a resolution range using Equation 7 of 145.3m. This indicates that two adjacent targets will be able to be detected correctly by radar if the distance between them is at least around 145.3m. Another result from Figure 1(c) is that M_{ML} is 1 and $M_{SL,0}$ is 0.0769 so that γ using Equation 9 is -11.14dB. According to the results in Figure 1(d), which is AF as a function of $t_d = 0$, it is obtained that the level of the main lobe touches the Doppler frequency axis for the first time at $f_D =$ ±0.0739MHz so that the velocity resolution using Equation 8 and $f_c = 10$GHz is 11077.5m/s. This indicates that two adjacent targets can be detected and differentiated correctly by radar if the velocity between them is at least 11077.5m/s.

For complete results and comparison with other B_n, see Table 5. It can be seen that the longer the bit length of this code, the sidelobe level decreases, resulting in a smaller PSLR. All PSLR values in Table 5 are still greater than the minimum PSLR required for radar applications, i.e., -30dB (Skolnik, 2002). Generally, increasing the bit length of the code results in an increase in time delay which results in a decrease in range resolution. On the other hand, increasing the bit length results in an increase in velocity resolution which is indicated by a smaller value.

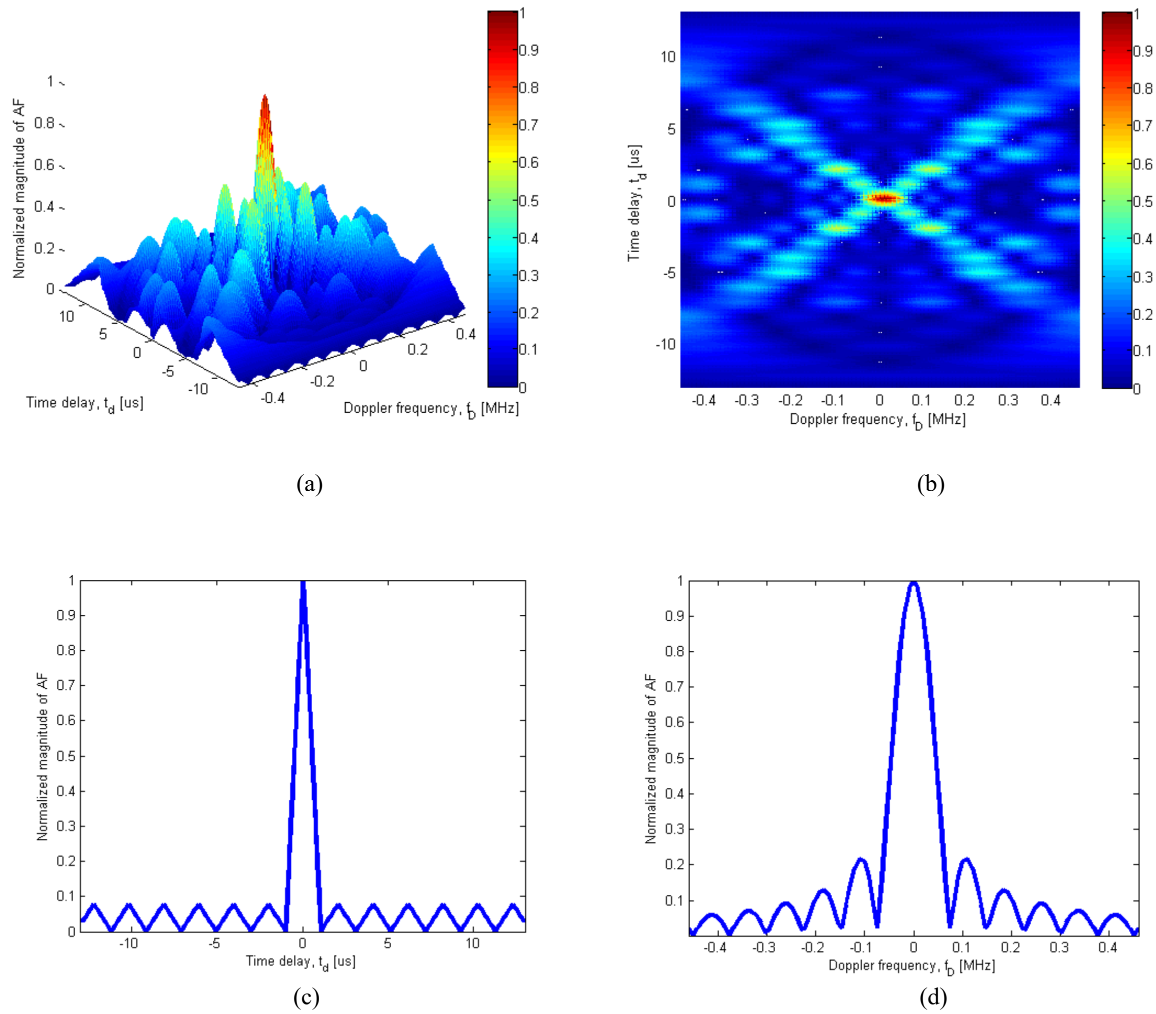

Figure 1. Ambiguity function from Barker code B_{13} for: (a) side view as function (t_d,f_D), (b) top view as function (t_d,f_D), (c) as function $f_D = 0$, and (d) as function $t_d = 0$

Table 5. Comparison of Range-Doppler Resolution and PSLR for Barker Code Variations

Type	t_d (μs)	f_D (MHz)	$M_{SL,0}$	SL_{min}	Δ_R (m)	Δ_V (ms^{-1})	γ (dB)
B_2	0.839	0.36	0.5	0.5	**125.8**	54000	-3.0103
B_3	1.452	0.16	0.4	0.4	217.8	24000	-3.9794
B_4	2.476	0.21	0.4	0.4	371.4	31500	-3.9794
B_5	1.508	0.12	0.32	0.32	226.2	18000	-4.9485
B_7	1.047	0.1371	0.1429	0.1429	157.1	20565	-8.4497
B_{11}	1.646	0.0546	0.1091	0.1091	246.9	**8182.5**	-9.6218
B_{13}	0.969	0.0739	0.0769	**0.0769**	145.3	11077.5	**-11.1396**

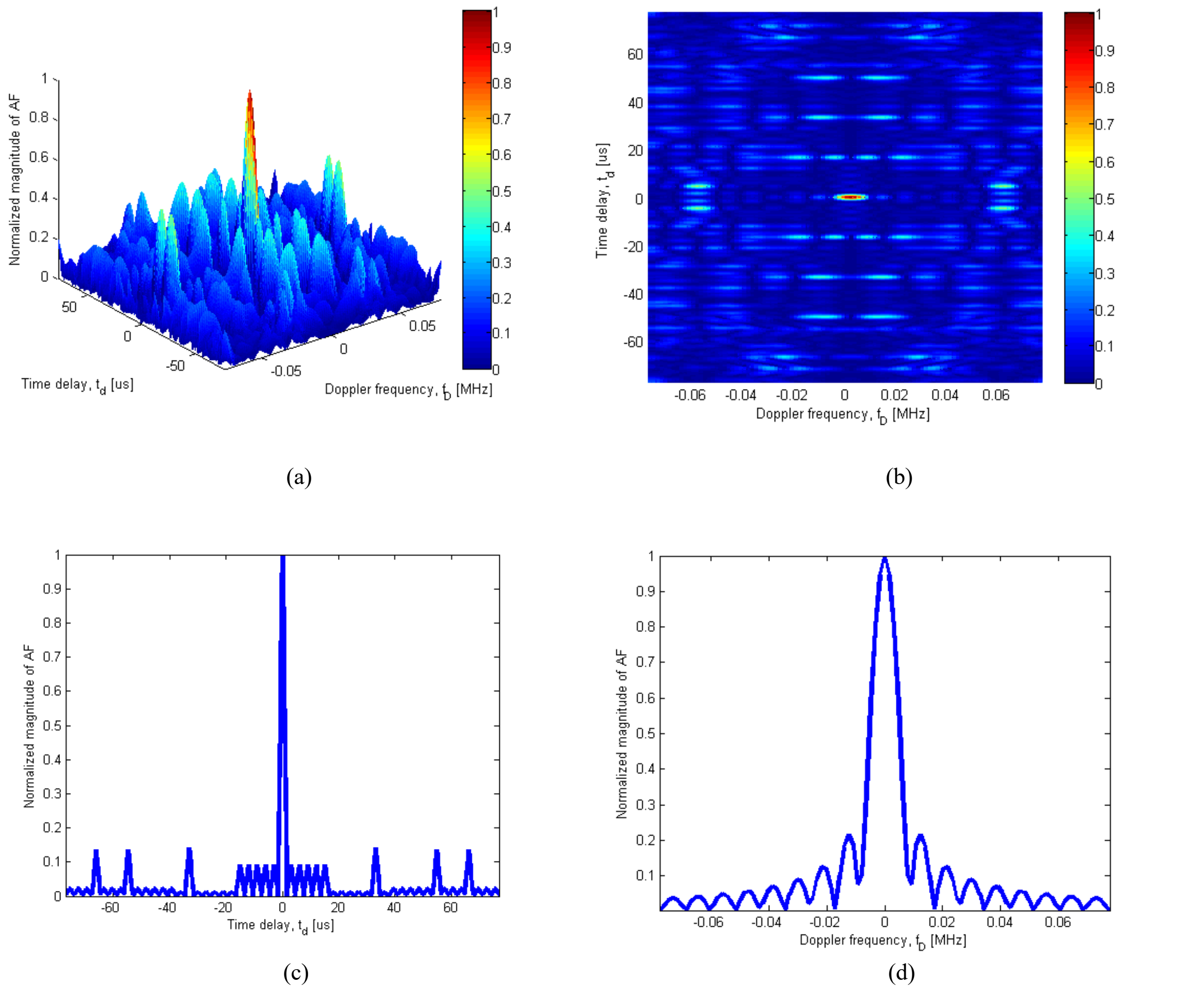

Figure 2. Ambiguity function from modified Barker code $B_{7,11}$ for: (a) side view as function (t_d,f_D), (b) top view as function (t_d,f_D), (c) as function $f_D = 0$, and (d) as a function $t_d = 0$

4.1.2. *Modified Barker Code with Itself*

For the AF performance results of the modified Barker code between Barker codes ($B_{m,n}$), an example is given for $B_{7,11}$ which is shown in Figure 2. Similar to the discussion in Figure 1, in Figure 2(c) we get $t_d = \pm 1.43\mu s$ and produces a range resolution of 214.5m. Another result from Figure 2(c) is that $M_{SL,0}$ is 0.0909 so that γ is -10.41dB. According to the results in Figure 2(d), where AF is a function of $t_d = 0$, $f_D = \pm 0.0094$MHz is obtained so that the speed resolution is 1402.65m/s. Complete results and comparisons with other $B_{m,n}$ are presented in Table 6. Since the Barker code was modified using itself, improvements were observed in the sidelobe levels, with several sidelobes significantly lower and more varied than those in the unmodified Barker code. If the Barker code without modification has the lowest sidelobe (SL_{min}) at B_{13} of 0.0769, then in the modified Barker code the level drops drastically, namely to SL_{min} = 0.00117 for $B_{11,7}$. This has a positive impact on increasing range resolution and Doppler resolution and also reducing PSLR. The PSLR values in Table 6 still meet the requirements for radar applications, i.e., -30dB (Skolnik, 2002). Thus, the Barker code modification can be applied to form a waveform that produces high and low range-Doppler PSLR resolution. When compared with Table 5, in Table 6 there is the smallest velocity resolution of up to 1402.65m/s compared to the lowest velocity resolution in Table 6 which is 8182.5m/s. The longer the bits of the modified Barker code, where one of the components is a Barker code with long bits, the greater the resolution range and velocity. On the other hand, the bit length of the constituent Barker code determines the level of resolution of the range-velocity and PSLR.

Table 6. Comparison of Range-Doppler Resolution and PSLR for Modified Barker Code Variations $B_{m,n}$

Type	Bit length (n)	t_d (μs)	f_D (MHz)	$M_{SL,0}$	SL_{min}	Δ_R (m)	Δ_V (ms^{-1})	γ (dB)
$B_{2,11}$	22	2.157	0.0273	0.0909	0.04545	323.55	4090.5	-10.4139
$B_{11,2}$	22	1.122	0.0273	0.5	0.03636	**168.3**	4090.5	-3.0103
$B_{3,13}$	33	1.45	0.0185	0.0769	0.03077	217.5	2769	**-11.1396**
$B_{13,3}$	33	1.45	0.0154	0.3333	0.02564	217.5	2307	-4.7716
$B_{5,13}$	65	1.207	0.0129	0.0769	0.01538	181.05	1938	**-11.1396**
$B_{13,5}$	65	1.207	0.0129	0.2	0.01538	181.05	1938	-6.9897
$B_{7,11}$	77	1.43	0.0094	0.0909	0.01299	214.5	**1402.65**	-10.4139
$B_{11,7}$	77	1.43	0.0094	0.1429	**0.00117**	214.5	**1402.65**	-8.4497

4.1.3. *Modified Barker Code with Hadamard Code*

For AF performance results from the modified Barker code with Hadamard code ($B_{m,}H_n$), an example of $B_{7,}H_8$ is shown in Figure 3. In Figure 3(c), td = ±0.9306μs and produces a range resolution of 139.59m. Another result from Figure 3(c) is that $M_{SL,0}$ is 0.75 so that γ = -1.2494dB. According to the results in Figure 3(d), f_D = ±0.0171MHz is obtained so the velocity resolution is 2571m/s. For complete results and comparison with other B_mH_n, they are shown in Table 7. Compared to the unmodified Barker code, the Barker code modified with the Hadamard code exhibits improved sidelobe levels, with several sidelobes significantly lower and more varied than those generated by the Barker code alone. For example, B_7H_8 has SL_{min} = 0.01786 compared to B_{13} which is 0.0769. This is good for increasing range resolution, Doppler resolution, and also reducing PSLR, there is even the smallest range resolution up to 123,285m compared to the range resolution in Table 5 and Table 6 where the lowest are 125.8m and 168.3m respectively. Based on these results, it has also been confirmed that the longer the bit length of the Barker code modified with the Hadamard code, the greater the resolution range and velocity. If you look at the PSLR values in Table 7, the PSLR is still greater than the minimum PSLR required for radar applications, i.e., -30dB (Skolnik, 2002).

Table 7. Comparison of Range-Doppler Resolution and PSLR for B_mH_n

Type	Bit length (n)	t_d (μs)	f_D (MHz)	$M_{SL,0}$	SL_{min}	Δ_R (m)	Δ_V (ms^{-1})	γ (dB)
B_5H_4	20	1.176	0.03	0.5	0.05	176.4	4500	-3.0103
H_4B_5	20	1.804	0.03	0.2	0.05	270.6	4500	-6.9897
B_7H_4	28	0.8219	0.0343	0.5	0.03571	**123.285**	5143.5	-3.0103
H_4B_7	28	1.26	0.0343	0.1429	0.03571	189	5143.5	**-8.4497**
B_5H_8	40	1.331	0.015	0.75	0.025	199.65	**2250**	-1.2494
H_8B_5	40	1.644	0.015	0.2	0.05	246.6	**2250**	-6.9897
B_7H_8	56	0.9306	0.0171	0.75	**0.01786**	139.59	2571	-1.2494
H_8B_7	56	1.15	0.0171	0.1429	**0.01786**	172.5	2571	**-8.4497**

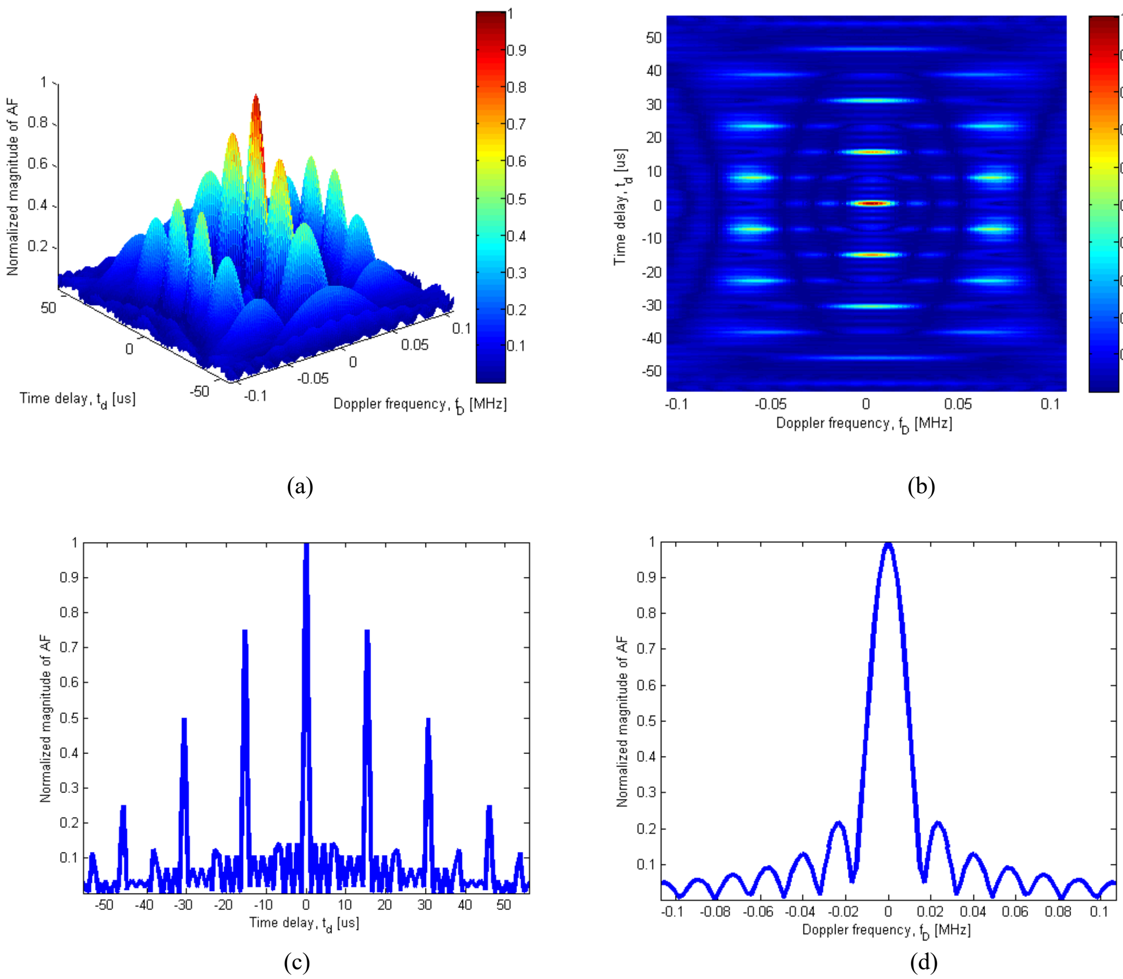

Figure 3. Ambiguity function from modified Barker code B_7H_8 for: (a) side view as function (t_d,f_D), (b) top view as function (t_d,f_D), (c) as function $f_D = 0$, and (d) as function $t_d = 0$

4.2. *AF Performance for Modified Barker Code in Radar Implementation*

Based on the same parameters in Table 4, the performance evaluation of AF for all possible modified Barker codes in Tables 2-3 is applied to the PA and the MIMO radars which are then compared with the performance of the SMIMO radar for the number of subarrays (K) is 5. Results of the performance comparison is summarized in Table 8 for mainlobe magnitude (ML), sidelobe magnitude (SL_0), and minimum sidelobe (SL_{min}). On the other hand, an example of a comparison of the AF performance of these radar variations is presented in Figure 4 with waveform conditions $B_{7,11}$. It can be seen that the AF results for the three types of radar, i.e., the PA, the MIMO, and the SMIMO ($K = 5$) where the AF obtained has differences in magnitude. The mainlobe magnitude of the AF on the three types of radar from the PA, the MIMO, and the SMIMO ($K = 5$) radars are 48.86dB, 53.86dB, and 54.75dB, respectively. The SMIMO configuration ($K = 5$) demonstrates superior AF performance compared to the two conventional radar types, as it leverages the AF properties of both PA and MIMO radars, combining directional coherent gain and waveform diversity gain. This supports the study reported by Tahcfulloh (2021). It can also be seen from Table 8 that displays the AF performance for all waveform variations where the AF performance of the MIMO and the SMIMO radars respectively increases by around 5dB and 6.28dB compared to the AF performance for the PA radar. These results confirm that the use of the Tx subarray affects the mainlobe-sidelobe AF magnitude and can even surpass the AF performance of conventional radars.

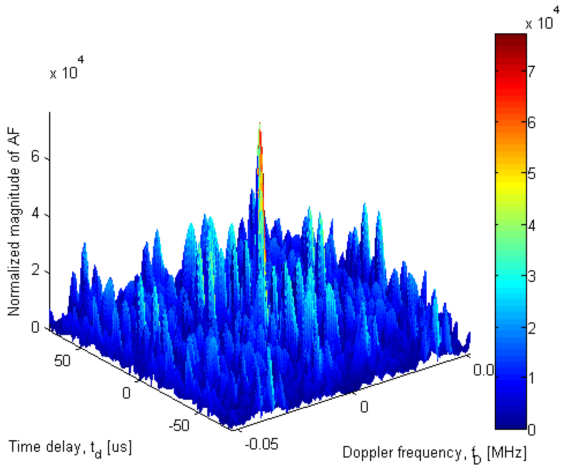

(a)

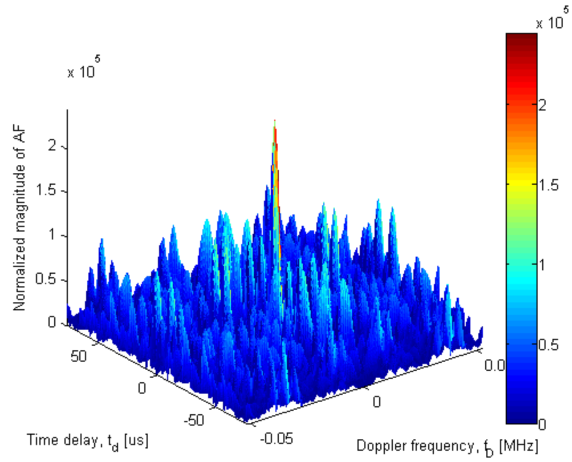

(b)

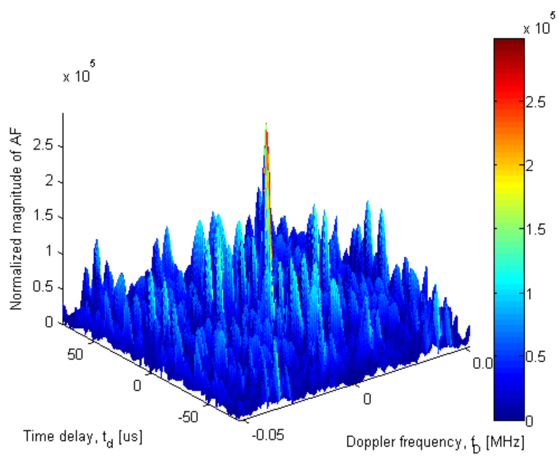

(c)

Figure 4. Comparison of AF performance using $B_{7,11}$ for radar: (a) PA, (b) MIMO, and (c) SMIMO (K = 5)

Table 8. Comparison of AF Performance of Modified Barker Code for Radar Variations

Type	PA			MIMO			SMIMO (K = 5)		
	ML (dB)	SL_0 (dB)	SL_{min} (dB)	ML (dB)	SL_0 (dB)	SL_{min} (dB)	ML (dB)	SL_0 (dB)	SL_{min} (dB)
$B_{2,11}$	43.42	33.01	30	48.42	38.01	35	49.3	38.39	35.88
$B_{11,2}$	42.72	40.41	30	48.42	45.41	34.03	49.3	46.29	34.91
$B_{3,13}$	45.91	34.77	30.79	50.91	39.31	35.79	51.79	40.65	36.67
$B_{13,3}$	45.91	41.14	29.54	50.91	46.14	35	51.79	47.02	35.88
$B_{5,13}$	48.13	36.99	30	53.13	41.99	35	54.01	42.87	35.88
$B_{13,5}$	48.13	41.14	30	53.13	46.14	34.54	54.01	47.02	35.88
$B_{7,11}$	**48.86**	38.45	30	**53.86**	43.45	35	**54.75**	44.33	35.88
$B_{11,7}$	**48.86**	40.41	30	**53.86**	45.41	35	**54.75**	46.29	35.88
B_5H_4	42.43	39.78	30	47.43	44.78	35	48.31	45.66	35.88

Type	PA			MIMO			SMIMO (K = 5)		
	ML (dB)	SL_0 (dB)	SL_{min} (dB)	ML (dB)	SL_0 (dB)	SL_{min} (dB)	ML (dB)	SL_0 (dB)	SL_{min} (dB)
H_4B_5	43.01	36.02	30	48.01	41.02	35	48.89	41.9	35.88
B_7H_4	44.47	41.46	30	49.47	46.46	35	50.35	47.34	35.88
H_4B_7	44.47	36.02	30	49.47	41.02	35	50.35	41.9	35.88
B_5H_8	45.55	44.77	30	51.02	49.77	34.54	51.38	50.27	35.42
H_8B_5	45.55	39.03	33.01	50.55	44.03	38.01	51.43	44.91	38.89
B_7H_8	**47.48**	46.23	30	**52.48**	50.85	35	**53.36**	52.11	35.88
H_8B_7	**47.48**	39.03	30	**52.48**	44.03	35	**53.36**	44.91	35.88

4.3. *Variation in Number of Tx Subarrays and its impact on AF Performance of SMIMO Radar*

Similar to the previous AF performance experiments which used the parameters in Table 4, the results obtained are shown in Table 9. This experiment was carried out to see the effect of variations in the number of Tx subarrays (K) of the SMIMO radar, i.e., K = 1, 2, ..., 10, on the AF performance of the modified Barker code either $B_{m,n}$ or B_mH_n. According to Tahcfulloh (2021), the SMIMO condition with K = 1 is associated as a PA radar, while for $K = N$ it is associated as a MIMO radar. SMIMO radar has optimum Tx-Rx gain and SINR performance at $K = [0.5*(M + 2)] + 1$ (Tahcfulloh, 2021). To prove that this also applies to AF performance, a transmission waveform in the form of a modified Barker code is applied. This suggests that by applying the modified Barker code waveform $B_{11,7}$, the AF performance results for this radar will have the level of mainlobe-sidelobe magnitude varying according to the number of Tx subarrays. AF results from this radar based on variations in the number of Tx subarrays (K) with $B_{11,7}$ is shown in Table 9.

Table 9. AF Performance of Modified Barker Code $B_{11,7}$ for Variation Subarray (K) of SMIMO Radar

K	ML (dB)	SL_0 (dB)	SL_{min} (dB)
1	**48.86**	**40.41**	**30**
2	51.65	43.20	32.78
3	53.15	44.70	34.29
4	54.11	45.66	35.25
5	54.75	46.29	35.88
6	55.14	46.69	36.28
7	**55.33**	**46.88**	**36.46**
8	55.28	46.83	36.42
9	54.91	46.46	36.05
10	**53.86**	**45.41**	**35.00**

For example, this radar for K = 5 (with M = 10) is presented in Figure 5 where the AF performance is expressed on a logarithmic scale which has a magnitude at the mainlobe (ML), first level sidelobe (SL_0), and minimum sidelobe (SL_{min}), i.e., 55.75dB, 46.29dB, and 35.88dB, respectively. It can be seen in Table 9 that as the number of Tx subarrays increases, the magnitude of the mainlobe-sidelobe for AF performance increases from K = 1 to K = 7 then decreases for K > 7. This is in line with the study reported by Tahcfulloh (2021) regarding Tx-R gain that for the total number of antenna elements in Tx and the total number of subarrays are M and K, respectively, the maximum Tx-Rx gain will be at $K = [0.5*(M + 2)] + 1$. Thus, for a SMIMO radar system with M = 10 elements, maximum AF performance is also obtained at K = 7 with ML, SL_0, and SL_{min} levels of 55.33dB, 46.88dB, and 36.46dB, respectively. It can also be seen in Table 9 that the mainlobe-sidelobe levels for K = 1 and K = 10 have the same AF performance as the mainlobe-sidelobe levels for the PA radar as the SMIMO (K = 1) and the MIMO radar as the SMIMO (K = 10) as in Table 8. This suggests that there is an advantage of the flexible SMIMO radar to condition the radar performance parameters based on the conditions of the detected target, where this capability is not available in previous radars such as the PA and the MIMO radars. Other results also show that if the mainlobe level is higher than the sidelobe level, it will have a positive influence on the PSLR value.

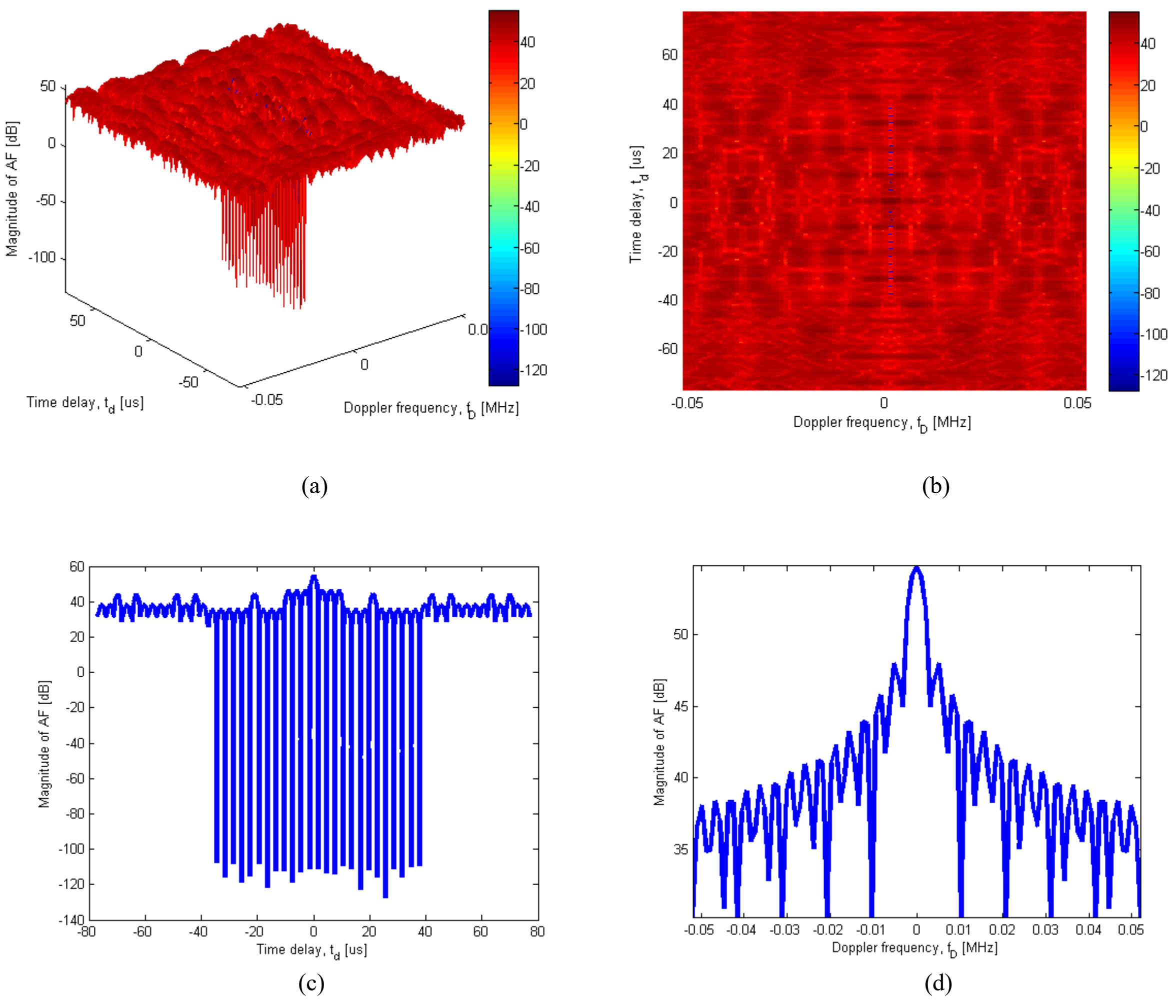

Figure 5. Ambiguity function in logarithmic scale from modified Barker code $B_{11,7}$ for: (a) side view as a function of (t_d,f_D), (b) top view as a function of (t_d,f_D), (c) as a function of f_D = 0, and (d) as a function of t_d = 0

5. Conclusion

This paper has presented the performance of AF for the modified Barker code with the Barker code itself and with the Hadamard code where the compromise of the combination has improved the AF performance of the original Barker code. The use of all these waveforms for radar systems such as PA, MIMO, and SMIMO radars and also to show the effect of variations in the number of antenna elements in the Tx subarray by taking into account various parameters including range resolution, velocity resolution, magnitude at mainlobe-sidelobe, and PSLR. The PSLR value formed from all waveform combinations has a PSLR value above the requirements for radar applications, i.e., above -30dB. The implementation of this waveform into a radar system provides an increase in the magnitude of the AF due to the processing gain by using the Tx subarray. The AF performance results for all waveform variations show that the AF performance of the MIMO and SMIMO radars respectively increases by around 5dB and 6.28dB compared to the AF performance for the PA radar. For M total antenna elements in the Tx array of the SMIMO radar will provide maximum AF performance with a certain modified Barker code at the number of subarrays K = 1+ 0.5*(M +2). This experiment shows the ability of the flexible SMIMO radar to adjust the number of antennas and the number of Tx subarrays to obtain AF performance that has the desired Δ_R, Δ_V, and PSLR so that targets can be detected well. In the future, it is hoped that there will be the formation of other modified transmission signals to this code to improve AF performance, especially PSLR, so that it can help and provide recommendations for radar designers to detect targets that are close to each other precisely and proportionally. To optimize AF performance and PSLR, choose code configurations based on radar environment and target characteristics. In high-clutter or interference settings, select codes like modified Barker or Hadamard to minimize sidelobe levels for improved detection. In low-clutter scenarios, opt for flexible codes offering higher range and velocity resolution. For closely spaced targets, prioritize codes that enhance range and Doppler resolution, such as modified Barker codes. When dealing with multiple targets at varying speeds, use combinations of Barker, Hadamard, or MIMO-based codes for fine resolution in both range and velocity.

References

Admaja, A. F. S. (2018). Pemetaan riset teknologi 5G. *Buletin Pos dan Telekomunikasi*, *16*(1), 27-40. https://doi.org/10.17933/bpostel.2018.160103

Aljalai, A. M. N., Feng, C., Leung, V. C. M., & Ward, R. (2020). Improving the Energy Efficiency of DFT-s-OFDM in Uplink Massive MIMO with Barker Codes. *2020 International Conference on Computing, Networking and Communications*, 731-735. https://doi.org/10.1109/ICNC47757.2020.9049829

Aziz, M. M., Habib, A., Maud, A. R. M., Zafar, A., & Irtaza, S. A. (2024). Anti-jamming radar waveform design for repeater jammer using reinforcement learning. *Vehicular Communications*, *47*. https://doi.org/10.1016/j.vehcom.2024.100768

Celik, O. O., & Tuncer, T. E. (2023). MIMO radar beampattern design by using Phased-Costas waveforms with PAR constraints employing a generalized ambiguity function. *Digital Signal Processing*, *135*. https://doi.org/10.1016/j.dsp.2023.103948

Chen, C. -Y., & Vaidyanathan, P. P. (2008). Properties of the MIMO Radar Ambiguity Function. *2008 IEEE International Conference on Acoustics, Speech and Signal Processing*, 2309-2312. https://doi.org/10.1109/ICASSP.2008.4518108

Dhawan, R., & Choudhary, A. (2023). Photonic generation of Barker encoded dual-nonlinear frequency modulated RADAR waveforms. *Results in Optics*, *13*. https://doi.org/10.1016/j.rio.2023.100583

Dong, B., Wang, Z., He, Y., Yang, A., & Qiao, Y. (2023). Long Distance Non-Line-of-Sight (NLOS) Optical Camera Communication based on the Barker Code Pilot. *2023 Opto-Electronics and Communications Conference*, 1-3, https://doi.org/10.1109/OECC56963.2023.10209585

Elayaperumal, S., & Hari, K. V. (2019). Optimal Irregular Subarray Design for Adaptive Jammer Suppression in Phased Array Radar. *2019 IEEE International Symposium on Phased Array System & Technology*. https://doi.org/10.1109/past43306.2019.902103

Farnane, K., & Minaoui, K. (2021). Analysis of the Radar Ambiguity Function for A New Golay Sets Shaping. *2020 10th International Symposium on Signal, Image, Video and Communications*, 1-4. https://doi.org/10.1109/ISIVC49222.2021.9487531

Friedlander, B. (2007). Waveform design for MIMO radars. *IEEE Transactions on Aerospace and Electronic Systems*, *43*(3), 1227-1238. https://doi.org/10.1109/TAES.2007.4383615

Han, K., & Hong, S. (2022). High-resolution phased-subarray MIMO radar with grating lobe cancellation technique. *IEEE Transactions on Microwave Theory and Techniques*, *70*(5), 2775-2785. https://doi.org/10.1109/TMTT.2022.3151633

Ilioudis, C. V., Clemente, C., Proudler, I., & Soraghan, J. (2016). Ambiguity Function for Distributed MIMO Radar Systems. *2016 IEEE Radar Conference*, 1-5.

Jiazhi, M., Longfei, S., & Jian, L. (2017). Improved Two-Targets Resolution Using Dual-Polarization Radar with Interlaced Subarray Partition. *2017 13th IEEE International Conference on Electronic Measurement & Instruments*. https://doi.org/10.1109/icemi.2017.8265831

Johnson, N., Chergui, M., Sternberg, O., Rockway, J. D., & Jones, W. L. (2016). Ambiguity Function Analysis for Passive Radar System Performance. *2016 IEEE Military Communications Conference*, 872-876. https://doi.org/10.1109/MILCOM.2016.7795439

Khan, W., Qureshi, I. M., & Sultan, K. (2014). Ambiguity Function of Phased–MIMO Radar With Colocated Antennas and Its Properties. *IEEE Geoscience and Remote Sensing Letters*, *11*(7), 1220-1224. https://doi.org/10.1109/LGRS.2013.2290010

Kim, D.-H., Kim, H.-J., & Lim, J.-H. (2021). Design of optimized coded LFM waveform for spectrum shared radar system. *Sensors*, *21*(17), 5796. https://doi.org/10.3390/s21175796

Lai, X., Zhang, X., Zheng, W., Li, J., & Zhou, F. (2024). Fragmented coprime arrays with optimal inter subarray spacing for DOA estimation: Increased DOF and reduced mutual coupling. *Signal Processing*, *215*. https://doi.org/10.1016/j.sigpro.2023.109273

Levanon, N., & Mozeson, E. (2004). *Radar Signals*. John Wiley & Sons.

Li, Y., Chang, S., Liu, Z., Ren, W., & Liu, Q. (2023). Range ambiguity suppression under high-resolution estimation using the MUSIC-AP algorithm for pulse-Doppler radar. *Signal Processing*, *214*. https://doi.org/10.1016/j.sigpro.2023.109237

Mahafza, B. R. (2002). *Radar Systems Analysis and Design Using MATLAB*. 4th Edition. Chapman and Hall/CRC.

Matsuyuki, S., & Tsuneda, A. (2018). A Study on Aperiodic Auto-Correlation Properties of Concatenated Codes by Barker Sequences and NFSR Sequences. *2018 International Conference on Information and Communication Technology Convergence*, 664-666. https://doi.org/10.1109/ICTC.2018.8539367

Ni'amah, K., Larasati, S., Hikmaturokhman, A., Amanaf, M. A., & Danisya, A. R. (2020). Coded random access technique based on repetition codes for prioritizing emergency communication. *Buletin Pos dan Telekomunikasi*, *18*(2), 145-158. https://doi.org/10.17933/bpostel.2020.180205

Nusenu, S. Y., Wang, W. -Q., & Basit, A. (2018). Time-modulated FD-MIMO array for integrated radar and communication systems. *IEEE Antennas and Wireless Propagation Letters*, *17*(6), 1015-1019. https://doi.org/10.1109/LAWP.2018.2829729

Riznvk, O., Tsmots, I., Noga, Y., & Myaus, O. (2021). Development of Adaptive Coding Means, Decoding of Data in Real Time Using Barker-Like Codes. *2021 IEEE 4th International Conference on Advanced Information and Communication Technologies*, 46-50. https://doi.org/10.1109/AICT52120.2021.9628911

Sabaria, S., & Tahcfulloh, S. (2024). Range and velocity resolution of linear-frequency-modulated signals on subarray-MIMO radar. *Jurnal ELTIKOM : Jurnal Teknik Elektro, Teknologi Informasi dan Komputer*. *7*(2), 200–209. https://doi.org/10.31961/eltikom.v7i2.940

Skolnik, M. I. (2002). *Introduction to Radar System*. 3rd ed. McGraw-Hill, 2002.

Sturm, C., & Wiesbeck, W. (2011). Waveform design and signal processing aspects for fusion of wireless communications and radar sensing. *Proceedings of the IEEE*, *99*(7), 1236-1259. https://doi.org/10.1109/JPROC.2011.2131110

Tahcfulloh, S. (2021). SMIMO radar: MIMO radar with subarray elements of phased-array antenna. *International Journal of Information Technology and Electrical Engineering*, *5*(2), 37-44. https://doi.org/10.22146/ijitee.58593

Tahcfulloh, S., & Hendrantoro, G. (2016). Phased-MIMO Radar Using Hadamard Coded Signal. *2016 International Conference on Radar, Antenna, Microwave, Electronics, and Telecommunications*, 13-16. https://doi.org/10.1109/ICRAMET.2016.7849573

Tang, L., Zhang, K., Dai, H., Zhu, P., & Liang, Y. -C. (2019). Analysis and optimization of ambiguity function in radar-communication integrated systems using MPSK-DSSS. *IEEE Wireless Communications Letters*, *8*(6), 1546-1549. https://doi.org/10.1109/LWC.2019.2926708

Wang, S., & He, P. (2018). Research on Low Intercepting Radar Waveform Based on LFM and Barker Code Composite Modulation. *2018 International Conference on Sensor Networks and Signal Processing*, 297-301. https://doi.org/10.1109/SNSP.2018.00064

Wei, W., & Wei, Y. (2023). Unimodular Sequence Set Design for MIMO Radar Ambiguity Function Shaping. *2023 IEEE Radar Conference*, 1-5. https://doi.org/10.1109/RadarConf2351548.2023.10149652

Wu, H., Jin, B., Xu, Z., Zhu, X., Zhang, Z., & Lian, Z. (2023). Waveform design and signal processing for integrated radar-communication system based on frequency diversity array. *Digital Signal Processing*, *133*. https://doi.org/10.1016/j.dsp.2022.103839